Prepublished copy

Nature Environment & Pollution Technology

This is a peer-reviewed prepublished version of the paper

Type of the Paper (Original Research, Review)

Comparative Analysis of CART and Random Forest Classifiers for LULC Mapping: A Case Study of Brahmani-Baitarani River Basin, India

Sonali Kadam[1†], Sangram Patil[2], Kavita Sawant[1], Sae Jamdade[1], Apurva Gadilkar[1], Chahal Ohri[1], Namrata Rathi[1] and Jotiram Gujar[3]

[1] Department of Computer Engineering, Bharati Vidyapeeth's College of Engineering for Women, Pune, Maharashtra, India

[2]Department of Civil Engineering, Bharati Vidyapeeth's College of Engineering, Lavale, Pune, Maharashtra, India

[3]Department of Chemical Engineering Sinhgad College of Engineering Pune, Maharashtra, India

†Corresponding author: Sonali Kadam; sonali.kadam@bharatividyapeeth.edu,

ORCID details of the authors: Sonali Kadam https://orcid.org/0000-0002-1306-4113

Sangram Patil https://orcid.org/0000-0001-5431-2630

Jotiram Gujar https://orcid.org/0000-0003-0472-1051

Key Words	Remote sensing imagery; NDVI; NDWI; Supervised classification; Environmental monitoring
DOI	https://doi.org/10.46488/NEPT.2025.v24i04.B4308 (DOI will be active only after the final publication of the paper)
Citation for the Paper	Kadam, S., Patil, S., Sawant, K., Jamdade, S., Gadilkar, A., Ohri, C., Rathi, N. and Gujar, J., 2025. Comparative analysis of CART and random forest classifiers for LULC mapping: A case study of Brahmani-Baitarani River Basin, India. *Nature Environment and Pollution Technology*, 24(4), p. B4308. https://doi.org/10.46488/NEPT.2025.v24i04.B4308

ABSTRACT

Land Use and Land Cover (LULC) classification is essential for monitoring environmental changes, managing resources, and planning sustainable development. Accurate classification, however, remains a challenge due to the diversity of landscapes and the computational demands of processing large datasets. Among various machine learning (ML) algorithms such as Convolutional Neural Networks (CNN), Support Vector Machines (SVM), Random Forest (RF), and Classification and Regression Trees (CART), RF and CART were chosen for this study due to their robustness, simplicity, and efficiency in handling complex LULC classification tasks. This research focuses on the Brahmani-Baitarani River basin, a region known for its environmental significance and susceptibility to land-use changes. Using remote sensing data from Landsat 8, Landsat 9, and Sentinel-2 satellites, a comparative analysis of RF and CART was conducted to evaluate their performance in LULC mapping. The datasets were processed and analyzed on the Google Earth Engine (GEE) platform, utilizing multi-temporal image data and advanced filtering techniques. The results reveal that RF consistently delivers higher classification accuracy compared to CART, making it a reliable choice

for LULC studies in dynamic and heterogeneous landscapes. By integrating high-resolution satellite imagery with ML algorithms, this study provides detailed insights into the spatial distribution of land use across the Brahmani-Baitarani basin. These findings have practical applications in urban planning, natural resource management, and environmental conservation, offering valuable information for decision-makers and researchers working to address global environmental challenges.

1. INTRODUCTION

Land Use and Land Cover (LULC) is therefore the manner in which human begins to use land and other features of the physical landscape. They form a basis of analyzing human socio-economic activities and their effects on earth regarding the physical planning of towns, cities and the general natural resource management. LULC alterations have impacts on ecosystems, climate, and resources (Rong & Fu 2023) for example in recent times the increase in frequency of global flooding events and that changes LULC (Kadam et al. 2024). These systems are critical for standardizing, categorizing and differentiating between the numerous forms of land that exist; as such, they are considered important tools of measurement in the context of environmental studies (Nedd et al. 2021). Some of the uses of mapping and spatial data are important in evaluating the land observations. Therefore, it is still difficult to properly assess classification systems, while their ability to follow the changes in the proposed land frequency remains rather high. Some of these drawbacks affect environmental monitoring and functioning as well as planning of environment activities.

The Brahmani-Baitarani River Basin was chosen because of its distinct environmental problems and high variability of LULC, making it an important area for land cover classification research. The river basin is subject to frequent floods, intensive land use change, and varied topography, making the area imperative for precise LULC mapping. The hydrological complexity of the basin also creates difficulties in the study of land dynamics, necessitating strong classification methods. Also, efficient LULC analysis is crucial for flood risk management, agricultural planning, and ecological protection in this area.

Random Forest (RF) and Classification and Regression Trees (CART) have received extensive comparison in LULC classification but this study focuses on regional-specific analysis in a complex river basin while examining various sampling methods including random sampling and stratified sampling. This research deviates from previous work by assessing how the algorithms succeed in handling uneven geographic terrains and sensitive hydrological areas. This research contributes fresh information about RF and CART performance in detecting seasonal and environmental impact on land cover classification despite limited investigation in past studies.

Satellite remote sensing (RS) is a central source of data essential for studying and mapping the Earth's surface. The availability and growing number of Remote Sensing data supported by improved and cheaper satellites inclusively, radiometric, spectral, spatial, and temporal resolutions which allow users to work with large numbers of time-series data (Tassi et al. 2020). However, this allows for greater accessibility due to the ability to break down components and perform separate computational requests at once, yet this comes at the cost of elevation of computational complexity and time. To help overcome these challenges, Google has developed one of the largest platforms based on

cloud called Google Earth Engine that demonstrates considerable results in recent years (Feng et al. 2022). Another is online geospatial platform, which provides utilization of crazy amount of geospatial data as well as a set of powerful online tools for computational and visual analysis. Researchers can either preprocess or directly download multi-temporal image data that satisfies certain filtering conditions through the GEE platform (Velastegui-Montoya et al.2023). After this, they can engage a number of machine learning algorithms in order to perform the LULC classification and analysis on-line (Loukika et al. 2023).

Using ML algorithms on remote sensing imagery on LULC classification has garnered significant interest recently. Unlike the limitations of human decipher, AI techniques can effectively identify subtle patterns(Mahajan et al. 2024; Mahajan et al. 2024). ML techniques are now widely used in different sectors like remote sensing technology, in smart agriculture etc. Supervised techniques encompass various algorithms, including Classification and Regression Trees (CART), Support Vector Machine (SVM), Spectral Angle Mapper (SAM), Fuzzy Adaptive Resonance Theory-Supervised Predictive Mapping (Fuzzy ARTMAP), Random Forest (RF), Mahalanobis Distance (MD), Radial Basis Function (RBF), Decision Tree (DT), Multilayer Perceptron (MLP), Maximum Likelihood Classifier (MLC), Naive Bayes (NB) and Fuzzy Logic (Maxwell, 2018).

Some of machine learning methods are more accurate than others in the classification of LULC. According to the review of previous studies it reveals that Artificial Neural Networks (ANN), Support Vector Machines (SVM) and Decision Tree have the potential to conduct the classification techniques. The results show that Random Forest (RF) performs better in general compared with other classification methods. Among all analyzed machine learning approaches, RF and CART were identified as the best-performing algorithms for LULC. classification that offers much accuracy than those of the other researchers (Carranza-García, 2019).

Many studies have been devoted to the comparison of various approaches to the classification using techniques of machine learning. These investigations are useful to provide information on the drawbacks and advantages of the approach in terms of appearance of LULC maps. In proposed research, authors aim to conduct a comparative study focusing on the performance of RF and CART using two distinct datasets: Dynamic WorldCover and the European Space Agency (ESA). By evaluating the success of these techniques, the intend to help formulate future research on the use of LULC mapping.

2. MATERIALS AND METHODS

2.1. Study Area

The Brahmani Baitarani area which shown in fig. 1 is located in eastern Odisha and between 83°55′ to 87°30′

east longitudes and 20°28′ to 23°38′ north latitudes. It starts from the highlands of Jharkhand and flows through Odisha to the Bay of Bengal. That can be written down as the length of the river = 799 km and 355 km (Indraja, G., 2024). The Baitarani River is one of the six major rivers from Odisha with an elevation range from 32 to 1024 m.

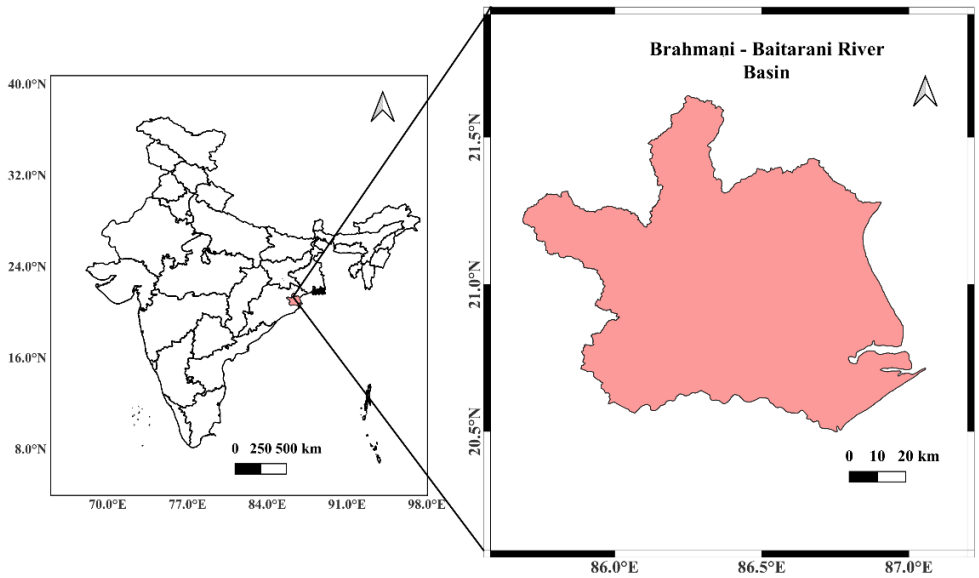

Fig. 1: Study Area

The major part of the region is covered with agricultural areas where the monsoon starts in June and extends till October.The southwest monsoon season (June to September) measures about 80% of yearly rainfall. The Baitarni sub-basin 1250- 1500 mm and Brahmani sub-basin receives 1250-1750 mm. Mean temperatures are 32°C (max) and 20°C (min). Recently occurred land use and climate changes have led to frequent flooding, damaging infrastructure and agriculture (Swain et al. 2021).

2.2. Satellite Data

Landsat-8, launched in 2013, provides medium-resolution imagery (30 meters) for land monitoring, urban mapping, and vegetation analysis. Landsat-9, launched in 2021, continues this mission with advanced technology, maintaining a 12-day revisit period and providing essential day data for continued land cover monitoring. Sentinel-2 L1C images, starting from June 27, 2015, with a 2–5-day revisit period, are also pivotal in this process.
Dynamic World Cover and LULC Data Dynamic World Cover offers near real-time LULC data with a 10-meter resolution, categorizing land into nine classes with probabilities (Brown et al. 2022). Using the Cloud Displacement Index, Directional Distance Transform, and S2 Cloud Probability, it achieves less than 35% cloud masking. This project, inspired by the 2017 World Cover conference and launched by the ESA, produces a global 10-meter resolution land cover map incorporating data from both Sentinel-1 and Sentinel-2 satellites, focusing on 11 land cover types with over 75% accuracy (Zanaga et al. 2020; Zanaga et al. 2022).

2.3. Methodology

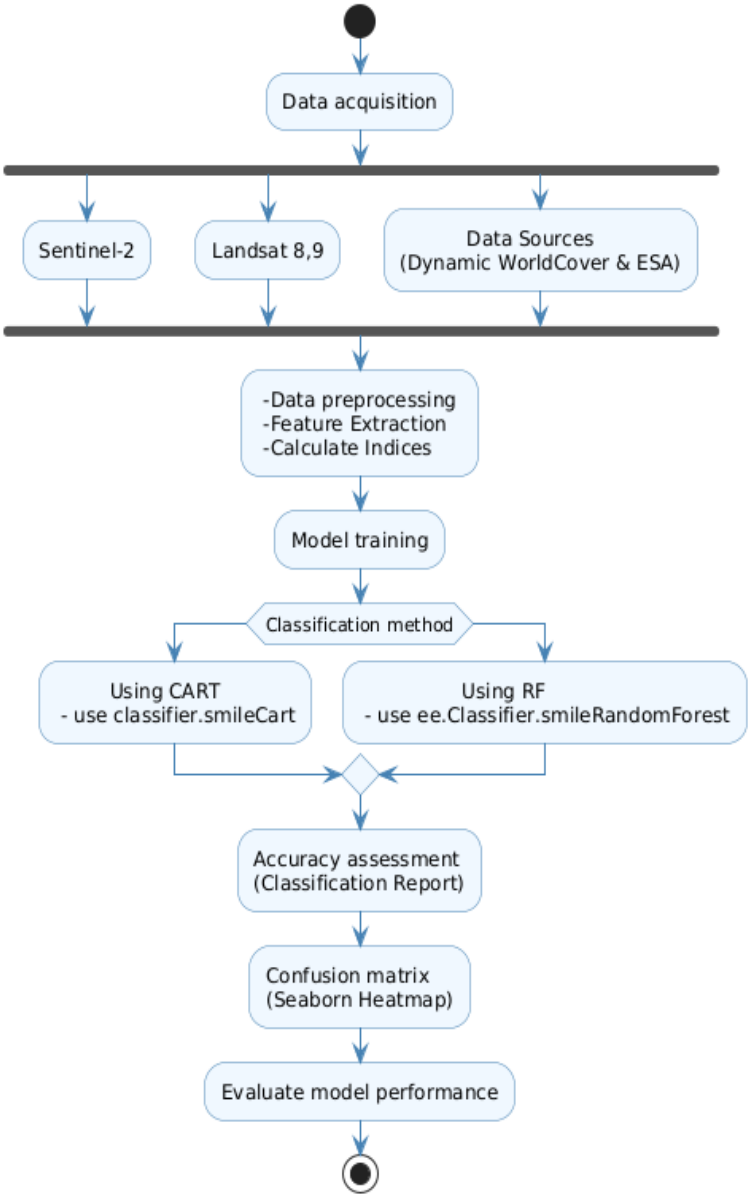

Fig.2: Methodology

The methodologies employed in this study are described in detail in the subsequesnt sections. The study aids in classifying the classification made by two Machine Learning algorithms Random Forest and CART in Fig.2.

2.3.1. Data Acquisition

The Sentinel 2 and Landsat data are being used to classify Land Use and Land Cover for the region of Brahamani and Baitarani. The underlying data is obtained from three different agencies to understand the difference in classification and the datasets. Sentinel 2 data can be collected from Dynamic WorldCover and the European Space Agency. The data consists of multispectral images, which undergo preprocessing techniques to remove

unnecessary noise or artifacts, cloud masking, or any geometric or atmospheric correction. From the segmented regions, we extract key spectral, textural, and contextual features. As part of this process, various indices are calculated, such as the Normalized Difference Vegetation Index (NDVI), Normalized Difference Water Index (NDWI), and Normalized Difference Built-up Index (NDBI). The derived parameters can further help in understanding specific land cover attributes (Zhao et al. 2024).

2.3.2. Pre-processing, Feature Extraction and Calculate Indices

Preprocessing involves many procedures to improve data quality before it is time for classification. First, Sentinel-2 and Landsat imagery are chosen as well as they cropped based on predefined shapefile for our region of interest (ROI). Cloud masking is the most particular part of satellite data. Cloud masking is removed means it removes the unwanted pixels. In this way the accuracy for land cover classification can be substantially enhanced by removing armful factors such as unreliable pixels caused by both clouds and tree foliage cover. It also guarantees that all spectral indices, such as: NDVI (Normalized Difference Vegetation Index), NDWI (Normalized Difference Water Index), and NBR (Normalized Burn Ratio) are computed from correctly classified land surfaces and noise (clouds or cloud shadows) excluded (Mateo-García et al. 2018).
The data is then further improved using geospatial formats, applying transformations and exporting images for analysis. These methods collectively make LULC classification results more reliable; deleting atmospheric distortions and unwanted features from the image together.

NDVI = (NIR - RED) / (NIR + RED)
NDWI = (GREEN - NIR) / (GREEN + NIR)
NBR = (NIR - SWIR) / (NIR + SWIR)

Vegetation index NDVI serves as a common tool which measures plant greenness through chlorophyll levels. The specific area's water content is measured by NDWI (Ashok et al.2021). Distinct features within a 3-band satellite image of a basin are identified using the NDVI technique. NDVI evaluates vegetative cover through the evaluation of wavelengths in near-infrared versus red bands which produces values between -1 to 1(Gebeyehu et al. 2019). Vegetation indices derived from these satellite images have been used to assess vegetation cover which also means a biophysical indicator of soil erosion. Formula used combine visible Red Band (RED) and near infrared reflectance (NIR) to determine NDVI.
It is applied by calculating the difference between green and near infrared reflectance by using NDWI technique to determine water bodies from within a 3-band satellite image. Areas of high moisture content are highlighted against context land features in this index. Likewise, the NBR index is used to monitor burned regions and vegetation health by comparing short wave and near infrared reflectance. The two indices derived from Sentinel 2 data improve the classification of water bodies and burned land improving the accuracy of LULC analysis and environmental monitoring (Tempa et al. 2024).

2.3.3. Model Training

In this study, the training process begins with the selection of training datasets derived from Sentinel-2 and Landsat 8/9 satellite imagery. Prior to utilization the datasets receive preprocessing treatments to achieve both quality and consistency standards. During model training and testing operations the dataset gets divided into two separate parts named training samples and testing samples. A random sampling and stratified sampling approach ensures this split. A distributed random value appears in each outcome column for every instance in the dataset. The distribution of data between training and testing emerges from the split ratio value which functions as a floating-point number spanning between 0 and 1. The split ratio establishes the specific portion of data which contributes to the training process.

When preprocessing finishes the system creates labeled training samples which identify unique LULC classes consisting of vegetation, water bodies and constructed regions. The RF and CART systems use these selected samples to establish their models.

RF implements an ensemble approach where it uses numerous decision trees that combine predictions to dr1ive better classification outcomes. CART implements a single decision tree approach that divides the dataset recursively based on threshold of features to identify LULC types. Both classifiers leverage trained data of extracted spectral and textural features alongside contextual features to optimally classify the different land cover types present in the study region.

2.3.4. Classification

2.3.4.1. CART

CART operates as a binary decision tree classifier, creating simple, logical if-then decisions. Research shows that people commonly use CART for remote sensing tasks particularly land use and land cover mapping as well as vegetation identification and land update monitoring. Other ML algorithm often take time in normalization of data, but CART does not require normalization. It evaluates input variables to determine, which provides the highest information gain, thus guiding node splits at each level (Shetty 2019). CART's robustness to noisy data and its ability to cope with split-outliers make the algorithm useful in a wider range of fields as this algorithm adapts some imperfections in data by adjusting splits to handle variance.

This method suits our study well, as high-resolution datasets are typically large, but the Cart software efficiently handles multiple datasets without affecting processing performance.

Research comparing classifiers shows that the CART classifier delivers equally accurate, if not superior, results compared to other common classification algorithms.In this study, we utilized the "classifier.smile-Cart" method for Land Use Land Cover classification.

2.3.4.2. Random Forest

Machine learning algorithms, such as Random Forest, have proven highly effective in analyzing intricate

remote sensing datasets. stratified Forest has a key advantage in handling large datasets with high-dimensional features. By using multiple decision trees, the Random Forest is more resistant to overfitting than individual decisions trees which contributes to its reliability, and it is able to classify complex patterns from satellite imagery (Mahendra et al. 2025). RF classifiers consist of multiple decision trees, where the final classification result is obtained through a voting process among these trees. The RF approach involves two types of random selection. Firstly, it randomly helps in creating subsets from the training dataset, representing a subtree that provides an individual classification result. The final result is then based on the aggregated votes from all these subtrees (Xie et al. 2019). Our study is focused on Land cover classification using ee.Classifier.smileRandomForest(). This algorithm builds 100 decision trees for the classification task, enhancing the overall accuracy androbustness of the predictions.

For this study area, it is particularly effective regionally due to diverse land cover types ranging from Urbanization to farmlands, rivers, forests, and water bodies. The multi-spectral images collected by Sentinel-2 and Landsat satellites combined with Random Forests have achieved comprehensive RF classification that really is detailed and accurate. It also makes it possible to map such detailed land-cover change information through time series data analysis. This is particularly important for monitoring the impact of land-use change on water resources, agriculture and the environment in this region.

2.3.5. Accuracy Assessment

In this research, accuracy assessment involves several key steps using machine learning tools and methodologies. Specifically, the sklearn.metrics module is utilized to calculate and print the classification report, accuracy score, and confusion matrix. The classification_report function provides a detailed breakdown of recall,precision and F1-score for each class. The accuracy_score function computes the overall accuracy of the model, which is the ratio of correctly predicted instances to the total instances. The confusion matrix, displayed using Seaborn's heatmap, offers a visual representation of the true vs. predicted classifications, helping identify misclassifications.

The formula for accuracy is expressed as:

Accuracy=Number of correct predictions / Total number of predictions

Additionally, the classifierMetrics function is designed to evaluate performance of model, highlighting the effectiveness of the Random Forest classifier in this context. The function receives the true labels (y_test) and predicted labels (y_pred), printing out the classification metrics.

2.3.6. Confusion Matrix

The confusion matrix is plotted to visually assess how well the model is performing across different clas

ses. This comprehensive assessment method ensures a robust evaluation of the classification results, providing insights into areas for potential improvement. Furthermore, the Random Forest classifier is trained and tested using a subset of the dataset, with cross-validation enhancing the reliability of the accuracy measurement.

Performance evaluation of classification decisions across different land cover categories occurs through the confusion matrix model. The Random Forest classifier exhibits high accuracy performance in particular land cover categories but shows misidentification behavior in selected classes. The classification accuracy for Water and Bare Ground reaches maximum levels since their spectral features enable clear discrimination from other classes. The classification of Flooded Vegetation and Grassland suffers from major misinterpreted areas because their spectral signatures have similar characteristics. The spectral characteristics of Crops align closely with Shrub & Scrub vegetation thus leading to their classification overlap. Somewhere misclassification occurs because some images show a mixture of urban structures together with vegetation elements. The classifier makes incorrect decisions because land cover types share similar spectral information and because some pixels contain multiple classes as well as cyclic changes in vegetation and water levels.

2.3.7. Performance Evaluation

In our research, we perform a comprehensive accuracy assessment of the classification results through a series of steps leveraging both GEE and the scikit-learn library. We use several key metrics such as the classification report, accuracy score, class distribution and confusion matrix to evaluate performance. The classification report provides recall, precision and F1-score for each class, giving a detailed overview about model's performance. The accuracy score is the ratio of correctly predicted instances to the total instances, provides a summary measure of the classifier's accuracy. The class distribution is shown in Table.1. The confusion matrix visually represents the true versus predicted classifications, highlighting areas of misclassification and allowing us to evaluate the classifier's performance comprehensively.

The scikit-learn functions classification_report, accuracy_score, and confusion_matrix are used to compute the classification metrics. Seaborn: heatmap to plot the confusion matrix gives intuitive sense of classifier performance. By performing these extensive calculations of accuracy, we will ultimately get a well-rounded view of just how well our approach in this specific case worked, as well as information on any concrete areas we can improve upon.

Table 1: Comparison of Area km^2 and Percentage of RF and CART.

Data set	Classes	RF		CART	
		Area km^2	Percentage	Area km^2	Percentage
Dynamic WorldCover	Vegetation	609.96	6.47	775.87	8.23
	Built	1.228.10	13.02	1,217.78	12.91
	Barren	331.56	3.52	512.22	5.43
	Water	326.79	3.47	559.95	5.94

3. RESULTS

3.1. CART

The CART algorithm was employed to categorize the study area into four major categories: vegetation, barren land, built-up area and water bodies. According to the classification results, water 710.07 km^2, trees 1,162.23 km^2, grass land 818.87 km^2, flooded vegetation 647.74 km^2, crops 2,433.10 km^2, shrub & scrub 965.40 km^2, built-up area 1,338.98 km^2, and bare ground 1,353.42 km^2. These results were observed by the Dynamic World Cover dataset using stratified sampling over a duration of 6 months. Similarly, good near comparable results were observed using the ESA dataset, as illustrated in Fig 3.1.a, 3.1.b, 3.1.c, 3.1.d.

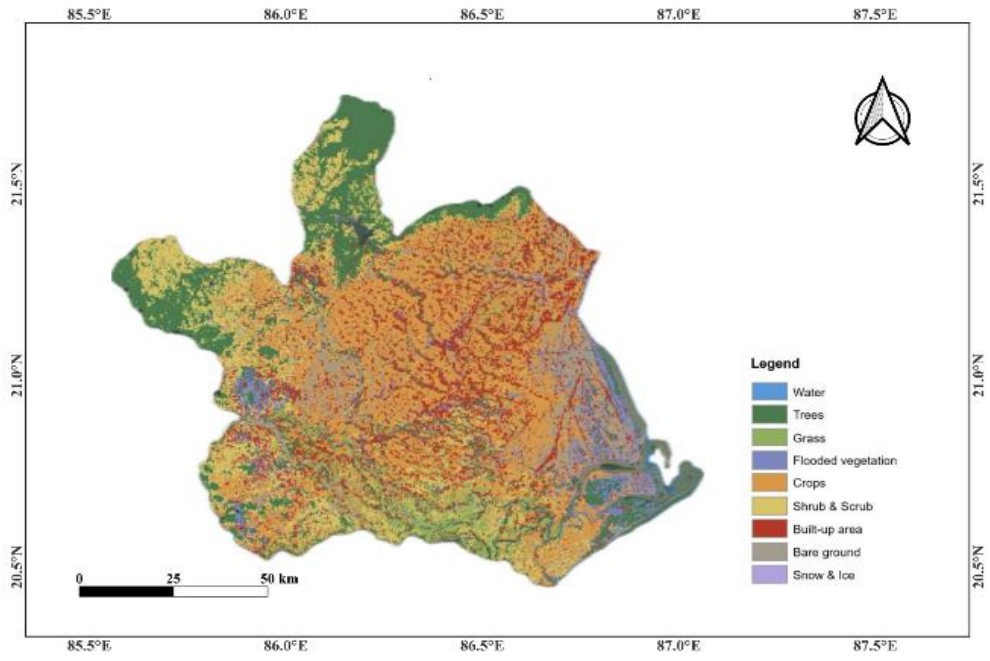

Dynamic World V1 2023

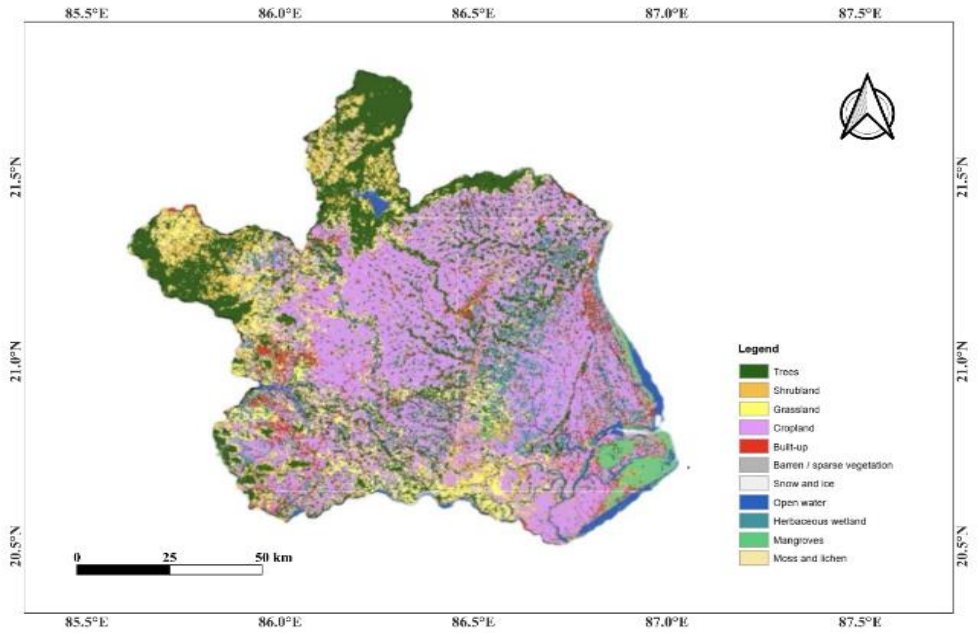

ESA WorldCover 10m v100/200 2023

Fig.3.1. a. Spatial distribution of LULC

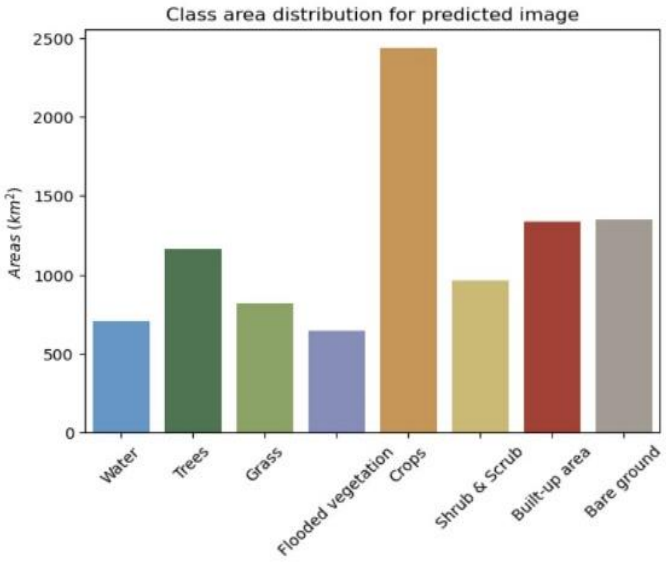

Dyanamic World V1 2023

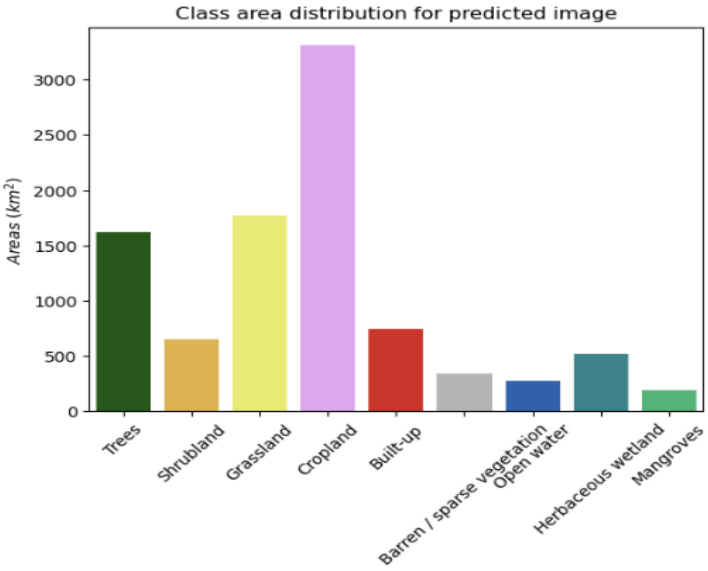

ESA WorldCover 10m v100/200 2023

Fig.3.1. b. Class distribution for LULC predicted image.

Classification report:

	precision	recall	f1-score	support
Water	0.71	0.69	0.70	291
Trees	0.58	0.57	0.58	330
Grass	0.55	0.60	0.58	286
Flooded vegetation	0.53	0.56	0.54	311
Crops	0.40	0.36	0.38	330
Shrub & Scrub	0.41	0.45	0.43	301
Built-up area	0.46	0.41	0.44	295
Bare ground	0.65	0.67	0.66	299
Snow & Ice	0.00	0.00	0.00	0
accuracy			0.54	2443
macro avg	0.48	0.48	0.48	2443
weighted avg	0.54	0.54	0.54	2443

Accuracy score: 0.54
[0, 1, 2, 3, 4, 5, 6, 7, 8]

Dynamic World V1 2023

Classification report:

	precision	recall	f1-score	support
Trees	0.64	0.65	0.64	296
Shrubland	0.56	0.52	0.54	304
Grassland	0.43	0.47	0.45	311
Cropland	0.64	0.58	0.61	305
Built-up	0.61	0.59	0.60	319
Barren / sparse vegetation	0.57	0.55	0.56	294
Snow and ice	0.00	0.00	0.00	0
Open water	0.79	0.80	0.79	304
Herbaceous wetland	0.55	0.55	0.55	300
Mangroves	0.74	0.85	0.79	269
Moss and lichen	0.00	0.00	0.00	0
accuracy			0.61	2702
macro avg	0.50	0.50	0.50	2702
weighted avg	0.61	0.61	0.61	2702

Accuracy score: 0.61
[0, 1, 2, 3, 4, 5, 6, 7, 8, 9, 10]

ESA WorldCover 10m v100/200 2023

Fig.3.1. c. Classification Report on LULC data prediction

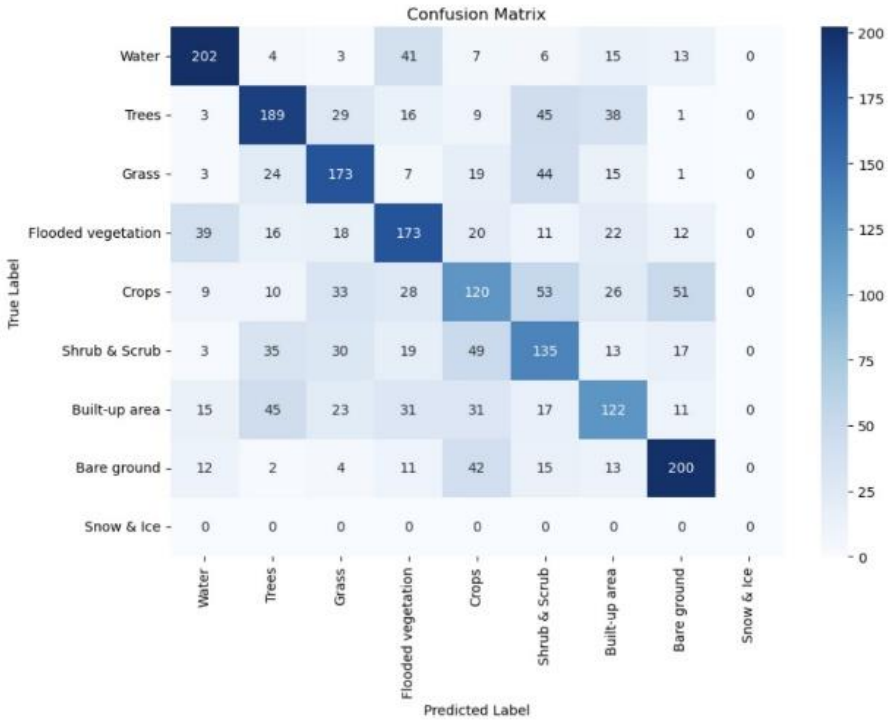

Dynamic World V1

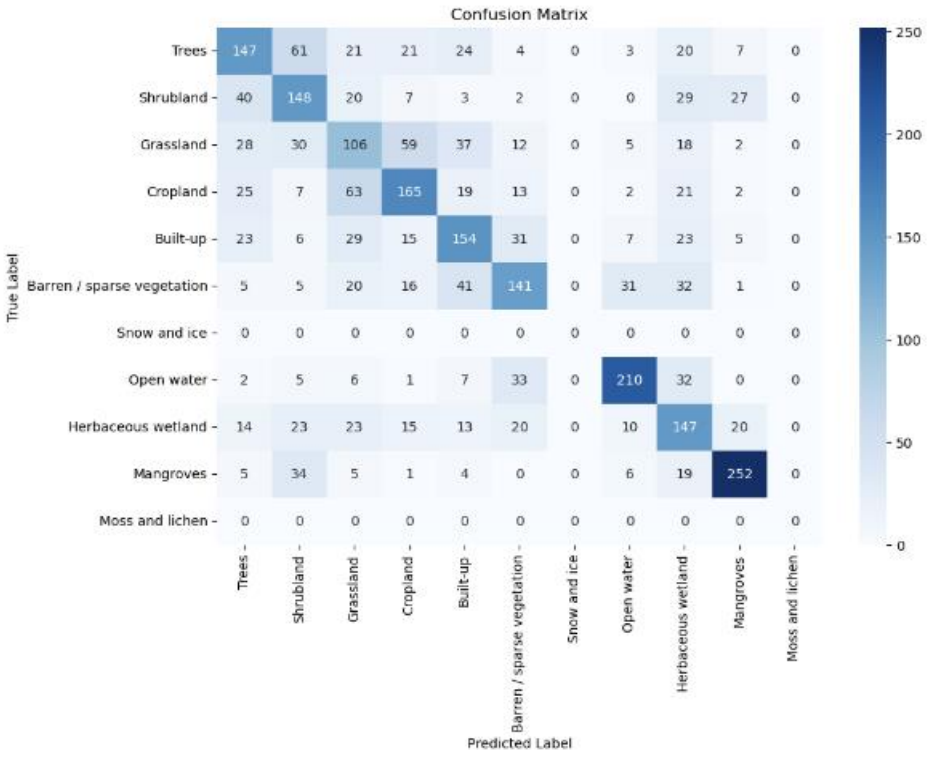

10m

ESA WorldCover v100/200

Fig. 3.1.d. Confusion matrix of LULC data prediction

3.2. Random Forest Algorithm

Fig 3.2.a, 3.2.b, 3.2.c, and 3.2.d depict the outcomes of a Random Forest classifier, utilizing stratified sampling of Dynamic World Cover and ESA data over a 6-month period with monthly classification. The land cover distribution in the Brahmani Baitarani basin is as follows: 330.36 km² of water, 1,193.78 km² of trees, 795.17 km² of grass, 637.55 km² of flooded vegetation, 2,908.39 km² of crops, 582.44 km² of shrub and crops, 1,570.72 km² of built-up areas, and 1,411.40 km^2 of

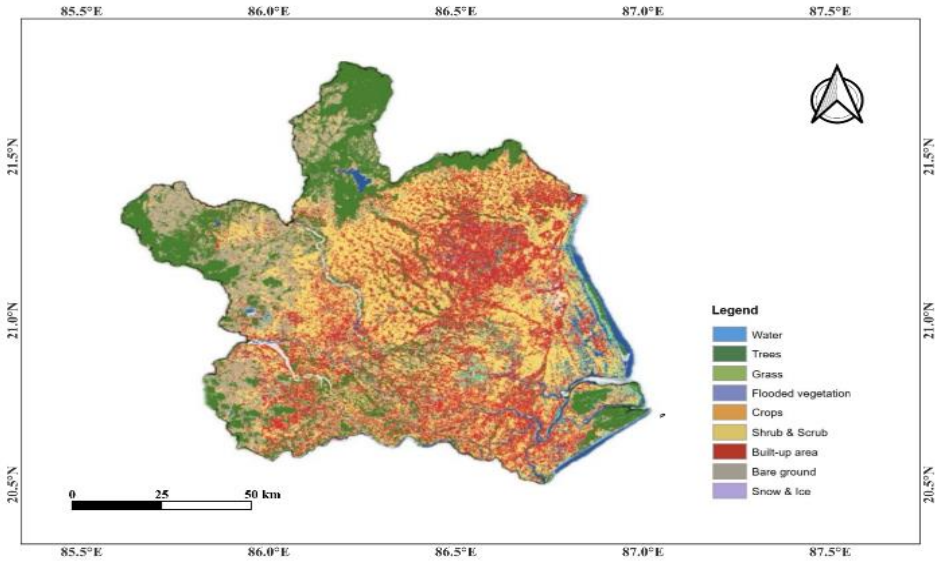

bare ground. Similar results were obtained using ESA dataset.

Dynamic World V1

ESA WorldCover 10m v100/200

Fig. 3.2.a. Spatial distribution of LULC

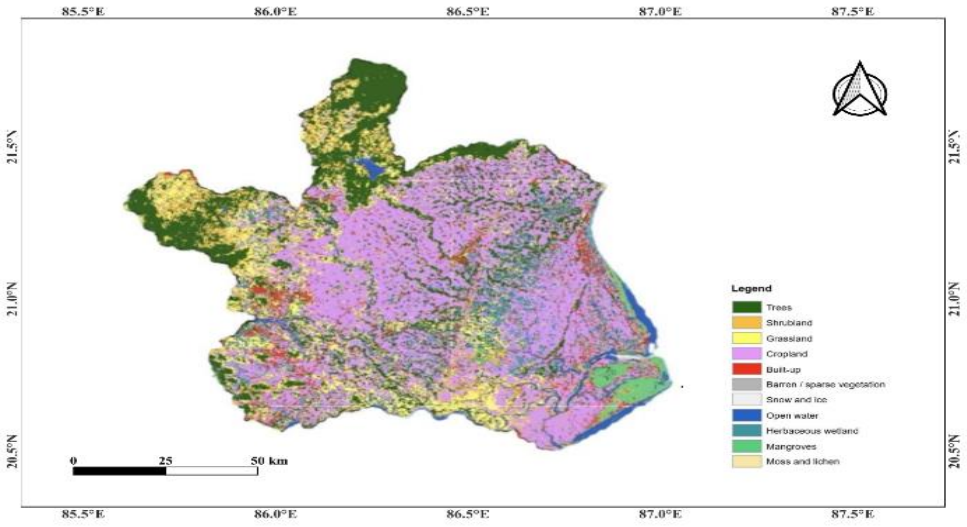

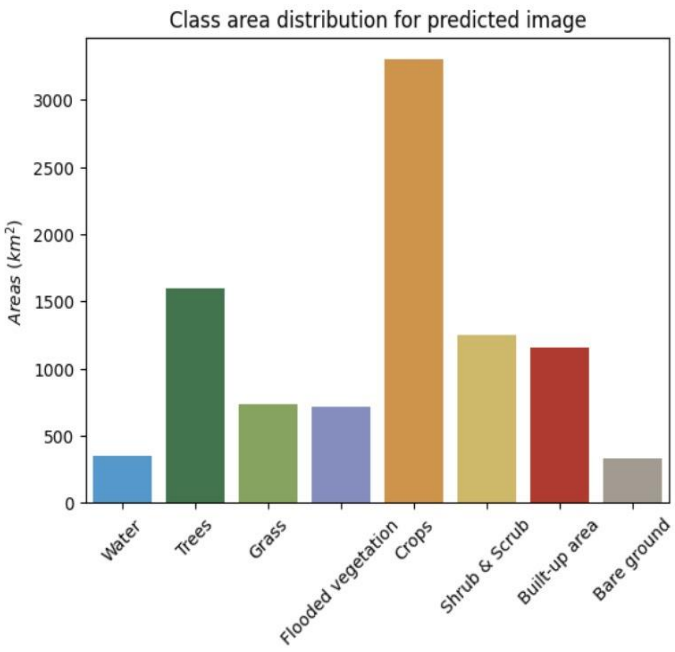

Dynamic World V1

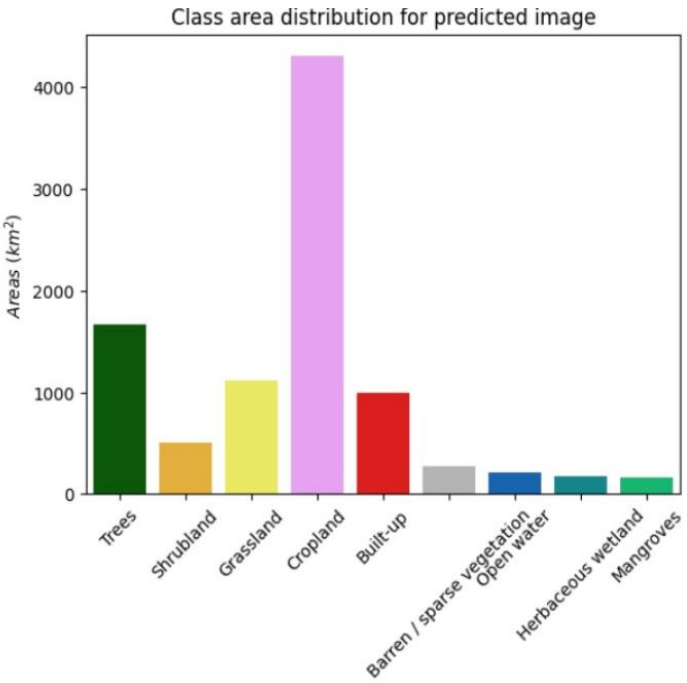

ESA WorldCover 10m v100/200

Fig.3.2. b. Class distribution for LULC predicted image

Classification report:

	precision	recall	f1-score	support
Water	0.85	0.69	0.76	291
Trees	0.72	0.68	0.70	330
Grass	0.66	0.77	0.71	286
Flooded vegetation	0.62	0.74	0.67	311
Crops	0.63	0.54	0.58	330
Shrub & Scrub	0.58	0.52	0.55	301
Built-up area	0.59	0.58	0.59	295
Bare ground	0.70	0.84	0.77	299
Snow & Ice	0.00	0.00	0.00	0
accuracy			0.67	2443
macro avg	0.60	0.59	0.59	2443
weighted avg	0.67	0.67	0.67	2443

Accuracy score: 0.67
[0, 1, 2, 3, 4, 5, 6, 7, 8]

Dynamic World V1

Classification report:

	precision	recall	f1-score	support
Trees	0.73	0.74	0.74	296
Shrubland	0.65	0.63	0.64	304
Grassland	0.62	0.51	0.56	311
Cropland	0.73	0.68	0.70	305
Built-up	0.66	0.75	0.70	319
Barren / sparse vegetation	0.61	0.78	0.68	294
Snow and ice	0.00	0.00	0.00	0
Open water	0.90	0.77	0.83	304
Herbaceous wetland	0.67	0.60	0.63	300
Mangroves	0.81	0.90	0.85	269
Moss and lichen	0.00	0.00	0.00	0
accuracy			0.70	2702
macro avg	0.58	0.58	0.58	2702
weighted avg	0.71	0.70	0.70	2702

Accuracy score: 0.70
[0, 1, 2, 3, 4, 5, 6, 7, 8, 9, 10]

ESA WorldCover 10m v100/200

Fig.3.2. c. Classification Report on LULC data prediction

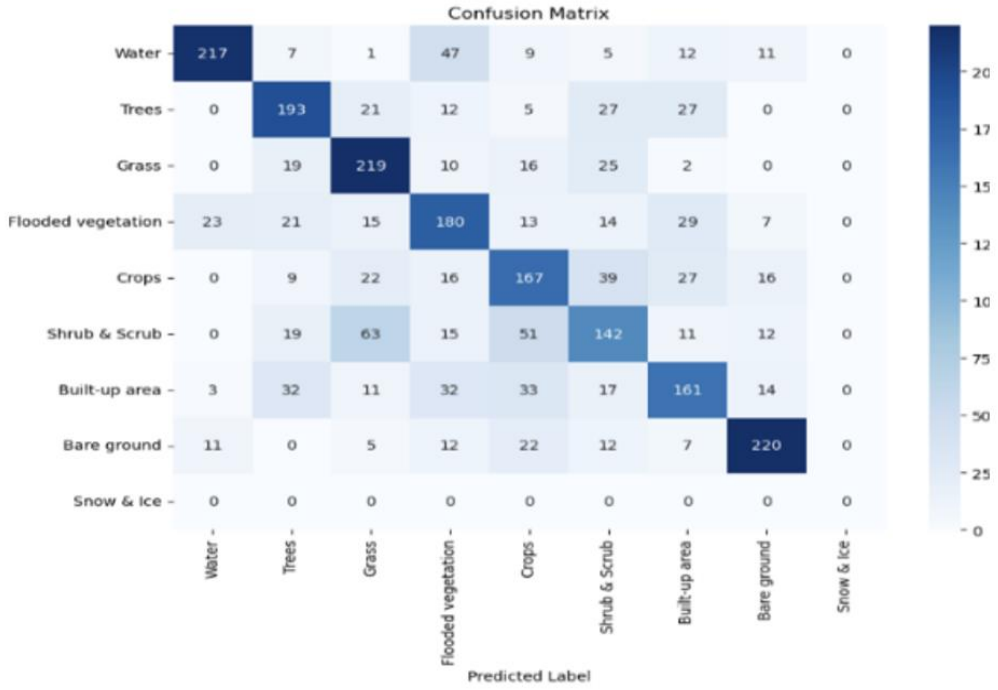

Dynamic World V1

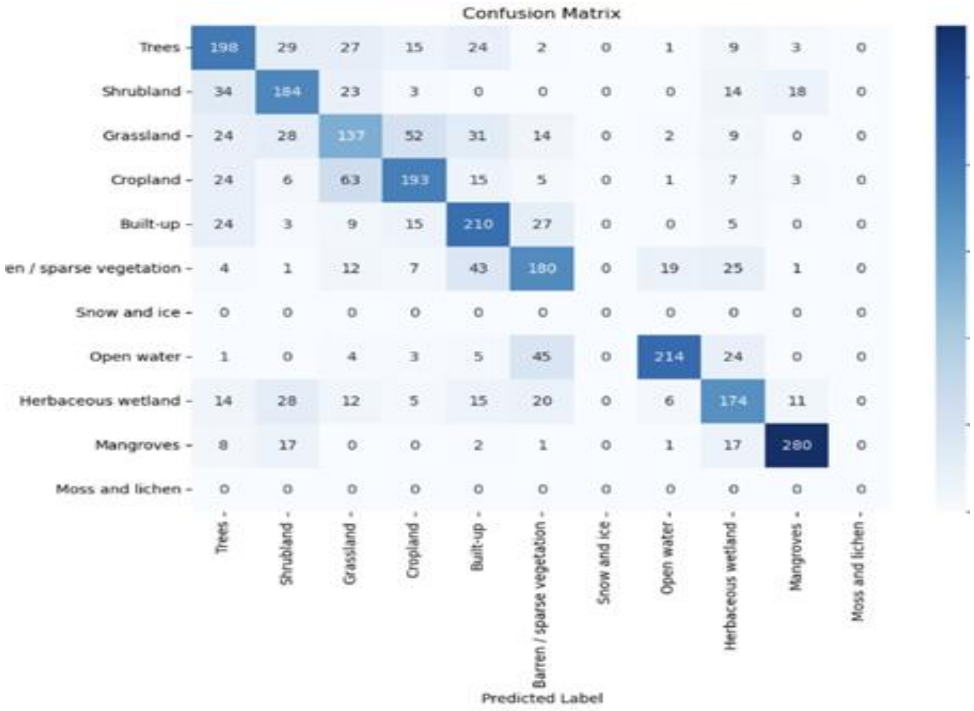

ESA WorldCover 10m v100/200

Fig. 3.2.d. Confusion matrix of LULC data prediction

3.1. Result Validation

For LULC classification, RF is preferred over CART, since RF has more accuracy and robustness than CART (Talukdar et al. 2020). In the Brahmani-Baitarani basin, RF outperformed the accuracy of CART. The Dynamic World Cover dataset classified 559 km² of water, 2,522 km² of crops and 1,217 km² of built-up areas with RF staying consistent over a six-month period. This ensemble method mitigates overfitting by averaging predictions over many decision trees, yielding more stable classifications, particularly in high-dimensional datasets like satellite imagery (Ren et al. 2024). The CART algorithm provided a satisfying accuracy, yet in our research, it displayed limitations common to decision trees, including susceptibility to small changes in the training data and overfitting. RF, on the contrary, showed ability to cope with noisy data and classified more complex land covers such as flooded vegetation and shrub area (trees 1397 km², flooded vegetation 775.87 km²) with higher accuracy. The performance of CART was limited by its lack of ensemble learning, which potentially renders RF a valid algorithm for mapping in our study area's land-use/land-cover (LULC). These findings demonstrate the significant benefits of employing RF for more accurate and consistent LULC classification, especially for diverse types of land.

4. DISCUSSION

The outcome of this research study demonstrates that Random Forest (RF) and Classification and Regression Trees (CART) which are ML algorithms, they exceed in achieving precise LULC classification. RF demonstrated robustness in classification in case of accuracy. The reasonable performance of CART was overshadowed by its propensity for overfitting which damaged the classification accuracy results. The research used Sentinel-2 together with Landsat 8/9 datasets alongside Dynamic WorldCover and ESA WorldCover which proven effective for classification purposes. The utilization of Google Earth Engine (GEE) simplified data analysis by providing smooth nonlinear processing for large-scale remote sensing image data. The preprocessing stage that involved cloud masking alongside geo-metric corrections and spectral index calculations of NDVI, NDWI and NDBI proved vital for achieving superior classification results.

The main result of this research demonstrates RF-based LULC classification can serve practical environmental objectives including environmental monitoring alongside urban planning and flood risk assessment and sustainable land management. Water resource management and disaster preparedness decisions benefit from precise LULC classification within the Brahmani-Baitarani River Basin because the region undergoes several land cover changes through monsoon-driven flooding. Aside from this, RF can offer government more effective zoning regulation, deforestation and agricultural land use tracking. Scientists can address issues of habitat destruction and loss of biodiversity by using data collected via RF-based classifications, as urban planners can integrate the information to implement infrastructure that is resilient and encourage green spaces.

A comparison with other studies proves that RF achieves better performance than CART in LULC, corroborating similar findings in Sentinel and Landsat studies. The classification accuracy of our study is fairly close to that has been reported previously which reinforces that RF is a robust algorithm for large-scale mapping. The performance

difference observed is primarily due to RF's capability for dealing with high-dimensional data while reducing variance through ensemble learning and the singularity of a CART tree that becomes much more sensitive to noise. Nevertheless, one of the drawbacks of Random Forest is its dependency on high-quality training data and sensitivity towards class imbalance, making it a better algorithm to use with continuous improvement of the dataset as well as hybrid modeling for better reliability.

5. CONCLUSIONS

The investigation carried out in the Brahmani Baitarani area emphasizes the necessity of combining higher order remote sensing approaches for the assessment of LULC classes. Our research demonstrated the effectiveness of categorizing the heterogeneous landscape using Landsat and Sentinel-2 satellite images, providing a better understanding of vegetation extent, built up areas, water bodies, and barren land in the study area. The findings therefore show that Random Forest has performed much better than the CART algorithm. This superiority could be attributed to the fact that RF uses an ensemble method of classifying features that helps it avoid overfitting, while at the same time improving the level of classification accuracy, especially in diverse and disaggregate land cover class. The classification report, confusion matrix, and other measures used in this chapter also give more refined accuracy estimation than the overall accuracy measure which confirms the ability of RF to handle high-dimensional data like the satellite imagery data.

In conclusion, this study provides a sound platform for environmental monitoring of the region as well as the application of sustainable land management practices in the Brahmani Baitarani area.

Author Contributions:

The methodology carried by Sae Jamdade and Chahl Ohri and investigation part by Sonali Kadam, while formal analysis conducted by Kavita Sawant. The original draft was prepared by Apurva Gadilkar, Sae Jamdade, Chahal Ohri, and Namrata Rathi. The review and editing process are done by Apurva Gadilkar and Namrata Rathi. Sangram Patil & Jotiram Gujar did supervision and project administration were managed by Sonali Kadam.

Acknowledgments:

The Authors thankfully acknowledge National Institute of Hydrology (NIH) for guidance and support.

REFERENCES

Ashok, A., Rani, H.P. and Jayakumar, K.V., 2021. Monitoring of dynamic wetland changes using NDVI and NDWI based landsat imagery. *Remote Sensing Applications: Society and Environment, 23,* p.100547. https://doi.org/10.1016/j.rsase.2021.100547

Brown, C.F., Brumby, S.P., Guzder-Williams, B., Birch, T., Hyde, S.B., Mazzariello, J., Czerwinski, W., Pasquarella, V.J., Haertel, R., Ilyushchenko, S. and Schwehr, K., 2022. Dynamic World, Near real-time global 10 m land use land cover mapping. Scientific Data, 9(1), pp.251. https://doi.org/10.1038/s41597-022-01307-4

Carranza-García, M., García-Gutiérrez, J. and Riquelme, J.C., 2019. A framework for evaluating land use and land cover classification using convolutional neural networks. Remote Sensing, 11(3), pp.274. http://dx.doi.org/10.3390/rs11030274

Feng, S., Li, W., Xu, J., Liang, T., Ma, X., Wang, W. and Yu, H., 2022. Land use/land cover mapping based on GEE for the monitoring of changes in ecosystem types in the upper Yellow River basin over the Tibetan Plateau. Remote Sensing, 14(21), pp.5361. https://doi.org/10.3390/rs14215361

Gebeyehu, A.E., Chunju, Z. and Yihong, Z., 2019. Assessment and mapping of land use change by remote sensing and GIS: A case study of Abaya Chamo Sub-basin, Ethiopia. *Nature Environment and Pollution Technology*, *18*(2), pp.549-554. https://neptjournal.com/upload-images/NL-68-28-(26)D-855.pdf

Indraja, G., Aashi, A. and Vema, V.K., 2024. Spatial and temporal classification and prediction of LULC in Brahmani and Baitarni basin using integrated cellular automata models. Environmental Monitoring and Assessment, 196(2), pp.117. https://doi.org/10.1007/s10661-023-12289-0

Kadam, S., Kadam, A., Devale, P., Bandgar, A., Manepatil, R., Kale, R., Gujar, J., Bundele, C. and Chavan, T., 2024, February. Improving Earth Observations by correlating Multiple Satellite Data: A Comparative Analysis of Landsat, MODIS and Sentinel Satellite Data for Flood Mapping. In *2024 11th International Conference on Computing for Sustainable Global Development (INDIACom)* (pp. 1581-1587). IEEE. https://doi.org/10.23919/INDIACom61295.2024.10498948

Loukika, K.N., Keesara, V.R. and Sridhar, V., 2021. Analysis of land use and land cover using machine learning algorithms on Google Earth Engine for Munneru River Basin, India. Sustainability, 13(24), pp.13758. https://doi.org/10.3390/su132413758

Mahajan, M., Kadam, S., Kulkarni, V., Gujar, J., Naik, S., Bibikar, S., Ochani, A. and Pratap, S., 2024. ECG signal classification via ensemble learning: addressing intra and inter-patient variations. *International Journal of Information Technology*, *16*(8), pp.4931-4939. https://doi.org/10.1007/s41870-024-02086-4

Mahajan, M., Kadam, S., Kulkarni, V., Gujar, J., Naik, S., Bibikar, S., Ochani, A. and Pratap, S., 2024, February. A Machine Learning Framework for the Classification of ECG Signals. In *2024 11th International Conference on Computing for Sustainable Global Development (INDIACom)* (pp. 264-270). IEEE. https://doi.org/10.23919/INDIACom61295.2024.10498810

Mahendra, H., Pushpalatha, V., Rekha, V., Sharmila, N., Kumar, D.M., Pavithra, G.S., Basavaraju, N.M. and Mallikarjunaswamy, S., 2025. LULC classification for change detection analysis of remotely sensed data using machine learning-based random forest classifier. https://doi.org/10.46488/NEPT.2025.v24i02.B4238

Mateo-García, G., Gómez-Chova, L., Amorós-López, J., Muñoz-Marí, J. and Camps-Valls, G., 2018. Multitemporal cloud masking in the Google Earth Engine. Remote Sensing, 10(7), pp.1079. http://dx.doi.org/10.3390/rs10071079

Maxwell, A.E., Warner, T.A. and Fang, F., 2018. Implementation of machine-learning classification in remote sensing: An applied review. International Journal of Remote Sensing, 39(9), pp.2784-2817. https://doi.org/10.1080/01431161.2018.1433343

Nedd, R., Light, K., Owens, M., James, N., Johnson, E. and Anandhi, A., 2021. A synthesis of land use/land cover studies: Definitions, classification systems, meta-studies, challenges and knowledge gaps on a global landscape. Land, 10(9), pp.994. https://doi.org/10.3390/land10090994

Ren, H., Pang, B., Bai, P., Zhao, G., Liu, S., Liu, Y. and Li, M., 2024. Flood Susceptibility Assessment with Random Sampling Strategy in Ensemble Learning (RF and XGBoost). Remote Sensing, 16(2), pp.320. https://doi.org/10.3390/rs16020320

Rong, C. and Fu, W., 2023. A Comprehensive Review of Land Use and Land Cover Change Based on Knowledge Graph and Bibliometric Analyses. Land, 12(8), pp.1573. https://doi.org/10.3390/land12081573

Shetty, S., 2019. Analysis of machine learning classifiers for LULC classification on Google Earth Engine. (Master's thesis, University of Twente). https://essay.utwente.nl/83543/1/shetty.pdf

Swain, S.S., Mishra, A., Chatterjee, C. and Sahoo, B., 2021. Climate-changed versus land-use altered streamflow: A relative contribution assessment using three complementary approaches at a decadal time-spell. Journal of Hydrology, 596, pp.126064. https://doi.org/10.1016/j.jhydrol.2021.126064

Talukdar, S., Singha, P., Mahato, S., Pal, S., Liou, Y.A. and Rahman, A., 2020. Land-use land-cover classification by machine learning classifiers for satellite observations—A review. Remote Sensing, 12(7), pp.1135. https://doi.org/10.3390/rs12071135

Tassi, A. and Vizzari, M., 2020. Object-oriented LULC classification in Google Earth Engine combining SNIC, GLCM, and machine learning algorithms. Remote Sens, 12(22), 1–17 https://doi.org/10.3390/rs12223776

Tempa, K., Ilunga, M., Agarwal, A. and Tashi, 2024. Utilizing Sentinel-2 Satellite Imagery for LULC and NDVI Change Dynamics for Gelephu, Bhutan. Applied Sciences, 14(4), pp.1578. https://doi.org/10.3390/app14041578

Velastegui-Montoya, A., Montalván-Burbano, N., Carrión-Mero, P., Rivera-Torres, H., Sadeck, L. and Adami, M., 2023. Google Earth Engine: A global analysis and future trends. Remote Sensing, 15(14), pp.3675. https://doi.org/10.3390/rs15143675

Xie, Z., Chen, Y., Lu, D., Li, G. and Chen, E., 2019. Classification of land cover, forest, and tree species classes with ZiYuan-3 multispectral and stereo data. Remote Sensing, 11(2), pp.164. https://doi.org/10.3390/rs11020164

Zanaga, D., Van De Kerchove, R., De Keersmaecker, W., Souverijns, N., Brockmann, C., Quast, R., Wevers, J., Grosu, A., Paccini, A., Vergnaud, S. and Cartus, O., 2021. ESA WorldCover 10 m 2020 v100, Zenodo [online]. https://doi.org/10.5281/zenodo.5571936

Zanaga, D., Van De Kerchove, R., Daems, D., De Keersmaecker, W., Brockmann, C., Kirches, G., Wevers, J., Cartus, O., Santoro, M., Fritz, S. and Lesiv, M., 2022. ESA WorldCover 10 m 2021 v200. https://doi.org/10.5281/zenodo.7254221

Zhao, Z., Islam, F., Waseem, L.A., Tariq, A., Nawaz, M., Islam, I.U., Bibi, T., Rehman, N.U., Ahmad, W., Aslam, R.W. and Raza, D., 2024. Comparison of three machine learning algorithms using Google Earth Engine for land use land cover classification. Rangeland Ecology & Management, 92, pp.129-137. https://doi.org/10.1016/j.rama.2023.10.007 .

NOMENCLATURE

ANN: Artificial Neural Networks

CART: Classification and Regression Trees

CNN: Convolutional Neural Network

DT: Decision Tree

ESA: European Space Agency

GEE: Google Earth Engine

LULC: Land Use Land Cover

MD: Mahalanobis Distance

ML: Machine Learning

MLC: Maximum Likelihood Classifier

MLP: Multilayer Perceptron

NB: Naive Bayes

NBR: Normalized Burn Ratio

NDBI: Normalized Difference Built-up Index

NDVI: Normalized Difference Vegetation Index

NDWI: Normalized Difference Water Index

NIR: Near Infrared Reflectance

RBF: Radial Basis Function

RED: Red Band

RF: Random Forest

RS: Remote Sensing

SAM: Spectral Angle Mapper

SVM: Support Vector Machine